

FEDSM-ICNMM2010-31089

DISSIPATIVE PARTICLE DYNAMICS SIMULATION OF NANO TAYLOR CONE

Meysam Joulaian¹

Soroush Khajepor²

Ahmadreza Pischevar³

Yaser Afshar⁴

^{1,2,3,4} Department of Mechanical Engineering, Isfahan University of Technology
Isfahan, 84156-83111, Iran

ABSTRACT

Dissipative particle dynamics (DPD) is an emerging method for simulating problems at mesoscopic time and length scales. In this paper, we present a new algorithm to describe the hydrodynamics of a perfect conductive fluid in the presence of an electric field. The model is based on solving the electrostatic equations in each DPD time step for determining the charge distribution at the fluid interface and, therefore, corresponding electrical forces exerted by the electric field to the particles near the interface. The method is applied to a perfect conductive pendant drop which is immersed in a perfect dielectric and hydrodynamically inactive ambient. We have shown that when the applied voltage is sufficiently high, the drop shape is changed to a cone with an apex angle which is near to the Taylor analytical estimation of 98.6° . Our results reveal that the presented algorithm gives new capabilities to the conventional DPD method for simulating nanoscale problems in the presence of an electric field.

Key words: DPD, Nano Taylor cone, electro hydro dynamic

I. INTRODUCTION

Recently, computational methods are becoming a rival for the experimental methods to probe complex phenomena in fluid

dynamics. With the aid of these methods, many details that cannot readily be captured by the experiment in a problem can be simulated. This becomes more significant when the problem length scales are reduced to micro or nano scales and therefore, the experiment expenses or limitations are raised drastically. There are a variety of computational methods; each appropriate for simulating problems with a specific range of time or length scales. Dissipative particle dynamics (DPD) is a new computational method which has been devised to simulate phenomena that their length scales lay in between continuum and atomistic level, i.e. mesoscopic length scales. This can happen in problems such as polymer adsorption [1], colloidal suspension [2, 3], binary immiscible fluids [4] or molecular biology [5].

Flexibility of DPD provides the possibility of studying the interest of hydrodynamics simulation in two-phase systems [6-8]. Clark et al. [6] studied the breakup and coalescence of droplets in an emulsion during processing with DPD method and showed that the method is capable of simulating the correct dynamics in multi-component, two-phase system. Also the simulation of free surface flows was included in DPD by tacking advantages of Many-bodies DPD (MDPD) [7-9].

In many multi-phase problems, electrostatic interactions can play a key role in the hydrodynamics behavior of the system. For example, the shape of drops can be changed in the

presence of an electric field which is important in processes like elector-spraying or electro-spinning. For simulating these systems with DPD, it is necessary to find a procedure to include long-range electric forces to the other DPD interactions. The aim of this paper is to explore a new algorithm for calculating forces applied by an electric field to the DPD particles of a perfect conductive fluid. The paper organized as follow: in section II we briefly review the DPD and MDPD formulation. In section III the electric field equations are explained. The algorithm for calculating the electrostatic forces of each DPD particles is presented in section IV. In section V some illustrative examples are given to validate the presented algorithm. Finally we conclude by a summary and conclusion.

II. MATHEMATICAL FORMULATION

Dissipative Particle Dynamics

DPD is a particle-based method in which each particle represents a cluster of atoms or molecules. The governing equation on the motion of these particles is Newton second's law:

$$\frac{\partial \vec{f}_i}{\partial t} = \vec{v}_i, \quad m_i \frac{\partial \vec{v}_i}{\partial t} = \vec{f}_i \quad (1)$$

The total force acting on each DPD particle, \vec{f}_i is a combination of three pair-wise forces: Conservative, Dissipative and Random forces [13]:

$$\vec{f}_i = \sum_j \vec{F}_{ij}^C + \vec{F}_{ij}^D + \vec{F}_{ij}^R \quad (2)$$

where sum runs over all neighbor particles. Neighbor particles refer to the particles that are placed in a certain distance, called cutoff radius, from a particle. If cutoff radius is denoted by R_c , then:

$$\vec{F}_{ij}^C = a_{ij} \omega^C(r_{ij}, R_c) \hat{e}_{ij} \quad (3)$$

$$\vec{F}_{ij}^D = -\gamma_{ij} \omega^D(r_{ij}, R_c) (\hat{e}_{ij} \cdot \vec{v}_{ij}) \hat{e}_{ij} \quad (4)$$

$$\vec{F}_{ij}^R = \sigma_{ij} \omega^R(r_{ij}, R_c) \theta_{ij} \delta t^{-1/2} \hat{e}_{ij} \quad (5)$$

Here $\vec{r}_{ij} = \vec{r}_i - \vec{r}_j$, $\hat{e}_{ij} = \vec{r}_{ij} / |\vec{r}_{ij}|$, $\vec{v}_{ij} = \vec{v}_i - \vec{v}_j$ and θ_{ij} is a random number drawn from a Gaussian statistics and has zero mean and unit variance. a_{ij} , γ_{ij} and σ_{ij} determine the strength of the conservative, dissipative and random forces, respectively. The weight functions are given by:

$$\omega^C = \omega^R = \sqrt{\omega^D} = \max\left[\left(1 - r_{ij}/R_c\right), 0\right] \quad (6)$$

Español and Warren [10] through the fluctuation-dissipation theorem showed, for thermal equilibrium, γ_{ij} and σ_{ij} should

obey: $\sigma^2 = 2\gamma k_B T$, where T is the system temperature and k_B is the Boltzmann constant.

Many-bodies DPD

The basic MDPD formulation is very similar to the standard DPD; the difference comes from the shape of conservative force where it is composed of attraction and repulsion parts; this force depends on the local density [8]:

$$\begin{aligned} \vec{F}_{ij}^C &= A \omega(r_{ij}, R_c) \hat{e}_{ij} & A < 0 \\ &+ B (\rho_i + \rho_j) \omega(r_{ij}, 0.75R_c) \hat{e}_{ij}, & B > 0 \end{aligned} \quad (7)$$

where the first term is the attraction and the second term is the repulsion part of conservative force. Here ρ_i is the instantaneous local density defined as:

$$\rho_i = \sum_j w(\vec{r}_{ij}, R_c) \quad (8)$$

where sum runs over all neighbor particles.

III. ELECTROSTATICS EQUATIONS

When a conductive fluid which can form a free surface or an interface with another fluid is subjected to an electric field, charges will be distributed at the fluid interface in order to create an equipotential surface and vanish the internal electric field. The presence of this interfacial charge will result in additional interfacial stress that opposes with the surface tension. In this case, the charges movement timescale in the fluid is determined by the electrical relaxation time defined as [11]:

$$\tau_e = \frac{\epsilon}{k} \quad (9)$$

where ϵ is the permittivity and k is the conductivity of the fluid. On the other hand, the fluid movement timescale is governed by the hydrodynamic relaxation time τ_h . In the case of a perfect conductive fluid, the conductivity of fluid goes to infinity and therefore, τ_e becomes negligible. Thus the electrical relaxation time is much smaller than the hydrodynamic relaxation time and the charges are screened instantly from the fluid by the external electrical field which can be calculated from the gradient of a scalar potential [11]:

$$\vec{E} = -\nabla V \quad (10)$$

V is the electric potential outside the fluid. In cases where the charge density is absent in the ambient region, the governing

equation for the electric potential is reduced to the Laplace's equation:

$$\nabla^2 V = 0 \quad (11)$$

Also the charge distribution ρ_s on the fluid surface is given by the Gauss's law [11]:

$$\rho_s = -\epsilon_0 E_n \quad (12)$$

where ϵ_0 is the permittivity of ambient, and E_n is the normal component of the electrical field at the interface given by:

$$E_n = \frac{\partial V}{\partial n} \quad (13)$$

Finally, the electrical force acting on the surface charges can be found from the Coulomb's law as [11]:

$$\vec{F}^e = \frac{\rho_s^2}{2\epsilon_0} d\vec{A} \quad (14)$$

where $d\vec{A}$ is outward normal to the interface.

IV. ADDING ELECTRICAL FORCES TO DPD FORCES

For a perfect conductive fluid, in each DPD time step, we can assume that the electrical field is in a quasi-static state since the electrical relaxation time is much smaller than the DPD time step. In the present work, the strategy used to include the electrical effects to the MDPD method consists of four basic steps:

Step 1: In each DPD time step, first we need to find the position of the fluid interface from the particles distribution. A common practice for finding the fluid interface profile is to divide the simulation domain into a finite number of cells and calculate the fluid density in each cell by considering the number of particles exist in each cell [6]. But this approach will not work properly during a single integration time step since it is very likely to lead to a cell with zero density within the fluid region when the cell size becomes smaller than the cutoff radius. Therefore, a different approach is adopted here in which the simulation domain is covered by a grid of finite nodes and the effects of particles are considered at each node with a weight function. This approach is very similar to the procedure used for the calculation of local density whereas the effects of neighbor particles are saved on a grid point instead of a particle. Therefore, the standard DPD weight function, which is used for calculating local density, can also be used for this purpose:

$$w(r_{ij}) = \max \left[\frac{15}{2\pi r_{eff}^3} \left(1 - \frac{r_{ij}}{r_{eff}} \right)^2, 0 \right] \quad (15)$$

where r_{ij} is the distance between particle i and node j , and r_{eff} is the effective radius. The criterion of deciding whether a node is located inside a fluid region or not, is the average local density ρ_{ave}^{node} . If one node has a local density greater than the average local density, then that node belongs to a fluid region. Here ρ_{ave}^{node} is defined as:

$$\rho_{ave}^{node} = \frac{1}{\alpha N} \sum_{i=1}^N \rho_i^{node} \quad (16)$$

where N is the number of nodes and α is the relaxation parameter. We have found $\alpha = 0.5$ result in a smooth profile for the fluid interface.

Step 2: Laplace's equation must be solved on the same domain (but only for the nodes located outside the fluid region) by appropriate boundary conditions. The electrical field and the charge density then can be calculated from Eq. (10) and (12), respectively.

Step 3: Knowing the charge density at the interface, electrical forces can be calculated from Eq. (14) for a cell. Therefore, it is necessary to redistribute this force over the DPD particles near the interface using an appropriate weight function. However, the weight function must prevent particles from collapsing on top of each others as reported by Groot. One possibility for the weight function which was previously used for the charge distribution is [12]:

$$f_i(r_i) = \max \left[\frac{3}{\pi R_e^3} \left(1 - \frac{r_i}{R_e} \right), 0 \right] \quad (17)$$

where R_e is the electrical cutoff radius and r_i is the particle distance from the interface. The distributed forces must be normalized such that the sum of all particles electrical forces leads to the same value of the cell electrical force:

$$F_i^e = \frac{f_i F_{Total}^e}{\sum_i f_i} \quad (18)$$

The electrical force on each DPD particle F_i^e must be added to the other DPD forces as:

$$\vec{f}_i = \vec{F}_i^e + \sum_j \vec{F}_{ij}^C + \vec{F}_{ij}^D + \vec{F}_{ij}^R \quad (19)$$

Step 4: At the final step, equation of motion integrated with the new forces. The velocity verlet (VV) algorithm is used for this purpose. The details about VV algorithm could be found elsewhere [13, 14].

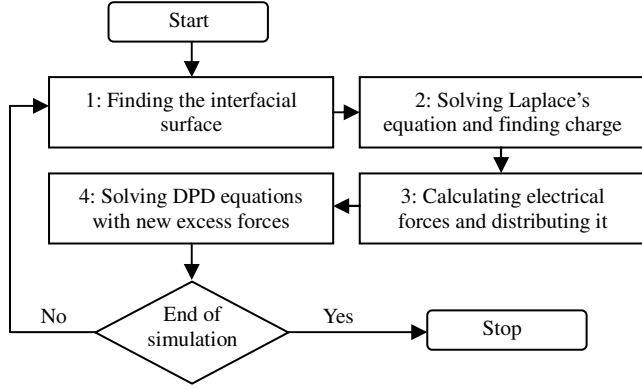


Figure 1: Algorithm for electrical force calculation

The above procedures are schematically shown in Fig. 1. In the following section the Taylor cone formation is simulated to validate the capabilities of the proposed algorithm.

V. TAYLOR CONE FORMATION

Taylor [15] analytically showed that when a pendant conductive liquid drop is subjected to a sufficiently strong electrical field, the drop shape is changed to a cone with an angle equal to 98.6° , known as Taylor cone.

As shown in Fig. 2, a system consists of a 3D nano droplet hanging from a metallic base is considered. The fluid is a conducting viscous liquid which is immersed in a perfect dielectric ambient with a known permittivity. The physical properties of fluid are given in Table 2. The simulation was performed in a $80 \times 80 \times 50$ DPD unit, periodic boundary box. The initial condition for the drop corresponds to a hemisphere with radius $R = 10$ which is pendant from a cylindrical base with the same radius and $t = 1$ thickness.

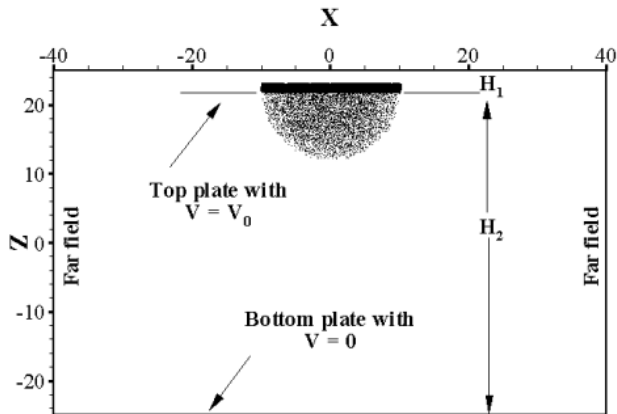


Figure 2: A liquid drop subjected to electrical field

Table 1: Simulation parameters used in the present study(DPD units)

	MDPD
density	6.05
random force amplitude (σ)	3.0
repulsion amplitude (A)	40.0
attraction amplitude (B)	-25.0
time step (δt)	0.02
H_1	3.0
H_2	47.0
$k_B T$	1.0

Drop protrudes a distance H_1 from the top of the simulation box to prevent particle interacting with the top boundary because of the periodic boundary conditions.

The effects of ambient drag force and the external pressure are negligible for this problem and therefore, it is rational to use MDPD method as a free surface model. The simulation parameters are summarized in Table 1.

To start the simulation, it is better to use an equilibrium distribution for the particles initial position. To achieve this goal, at the beginning a $20 \times 20 \times 20$ unit periodic boundary box is considered and filled with 48400 randomly positioned DPD particles. These particles are allowed to interact with each other through MDPD forces. The simulation is run for several thousand time steps to ensure equilibrium distribution of the particles. Then, a part of these particles are selected as the initial drop and the base. For this simulation, the drop and the base are made from 12645 fluid particles and 1907 frozen particles, respectively. Frozen particles take part in the interactions exactly in the same manner as the fluid particles, but their positions are retained during the simulation by removing them from the integration algorithm.

The domain boundaries for the potential Laplace's equation are considered to be the same as the simulation box, except for the top boundary. This boundary, like the drop was protruded a distance H_1 from the top of the simulation box. The boundary conditions for the electrical potential are:

$$V = V_0 \quad \text{On top boundary \& drop surface} \quad (20)$$

$$V = 0 \quad \text{On the bottom boundary} \quad (21)$$

$$\frac{\partial V}{\partial n} = 0 \quad \text{On the far field boundaries} \quad (22)$$

The far field boundaries must be chosen sufficiently far from the drop to prevent influences on the potential distribution near the drop. Here, this distance is chosen to be four times of the drop radius.

In order to solve the Laplace's equation with the mentioned boundary conditions, the MUDPAK 5.1 solver [16] is used. MUDPAK is a tested and documented solver for solving a

variety of PDE equations. This solver attempts to compute the second and fourth order accurate finite difference approximation of a 3D linear non-separable elliptic partial differential equation over a box domain. The number of meshes required for solving Laplace's equation is studied systematically to obtain the mesh-independent solution. We have found that if the divisions in the x and y directions were $\Delta x = \Delta y = 0.833$ and in the z direction $\Delta z = 0.489$, the solution would become insensitive to the further increase in the number of meshes.

The obtained result for the dimensionless potential field V/V_0 is depicted in Fig. 3 for a case where the top boundary is held at $V_0 = 80$ in DPD units. As we can see in this figure, the potential is approximately uniform near the bottom boundary while it curves toward the drop at the proximity of the top boundary.

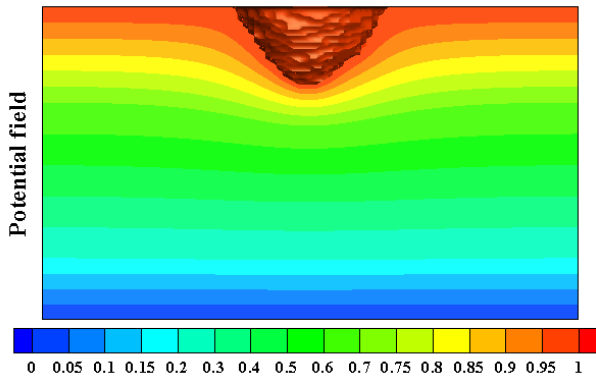


Figure 3: Dimensionless potential distribution

At the beginning of simulation, electrical field is switched off i.e. $V_0 = 0$ and the simulation is run for several hundred steps toward the equilibrium. After that, the upper boundary's voltage changed to initial value i.e. $V_0 = 1$ and the system is allowed to reach a new equilibrium point again. Then, the upper boundary's voltage is increased in small increments while the system allows reaching to its new equilibrium state. In each DPD time step, particles at the surface is detected and electric force applied to them. These particles are depicted in Fig. 4 at a typical time step. As we can see in this figure, the charged particles are placed on a thin layer near the drop surface.

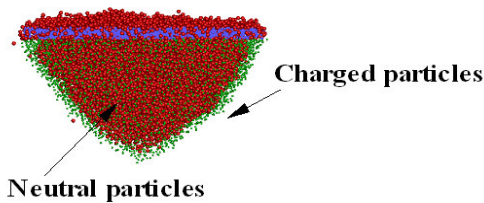


Figure 4: Charges distributed on a thin layer near the surface

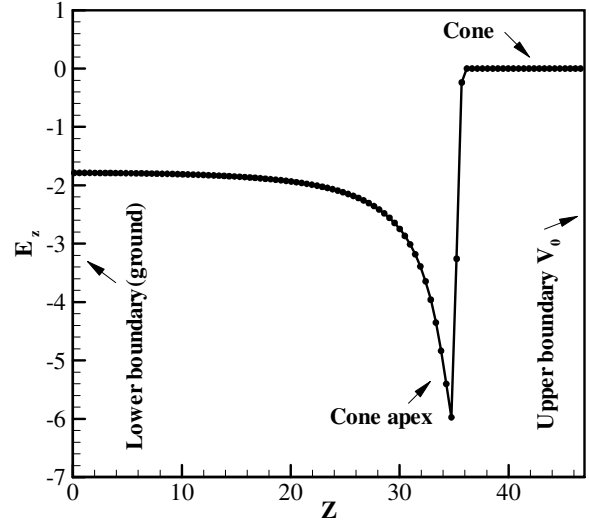


Figure 5: Electric field intensity near the cone's tip

The electrical field also is calculated by a second order finite difference approximation of Eq. (10). Fig. 5 depicts the electrical field in the z direction, E_z , when the Taylor cone is formed. The maximum absolute value in E_z corresponds to the cone apex where the charge density is maximum.

As the applied voltage V_0 is increased, the shape of drop deviates from its initial spherical shape and converges to a cone to increase the interface curvature and balancing the excessive generated electrical stresses at the drop surface. This trend is depicted in Fig. 6. As we see in this figure, when the voltage becomes high enough, a Taylor cone with an angle of 98.6° is formed. After this critical voltage, the cone becomes unstable and finally inclines to drive a jet.

We note that the significant dimensionless numbers in a two-phase system are the Reynolds number, Capillary number, Weber number and Ohnesorge number. In the case of a stationary drop, the Ohnesorge number (Oh) becomes a dominant dimensionless number [17]. This number expresses the ratio of viscous force to the surface tension force.

$$Oh = \frac{\mu}{\sqrt{\rho R \Gamma}} \quad (23)$$

where μ is the drop viscosity, Γ is the surface tension, ρ is the density and R is the drop radius. Oh number and the related parameters are summarized in Table 2 where DPD parameters are selected as Table 1 for water. By matching Oh number in DPD system to its corresponding value in the real physics, the radius of the simulated water drop is found to be $221nm$.

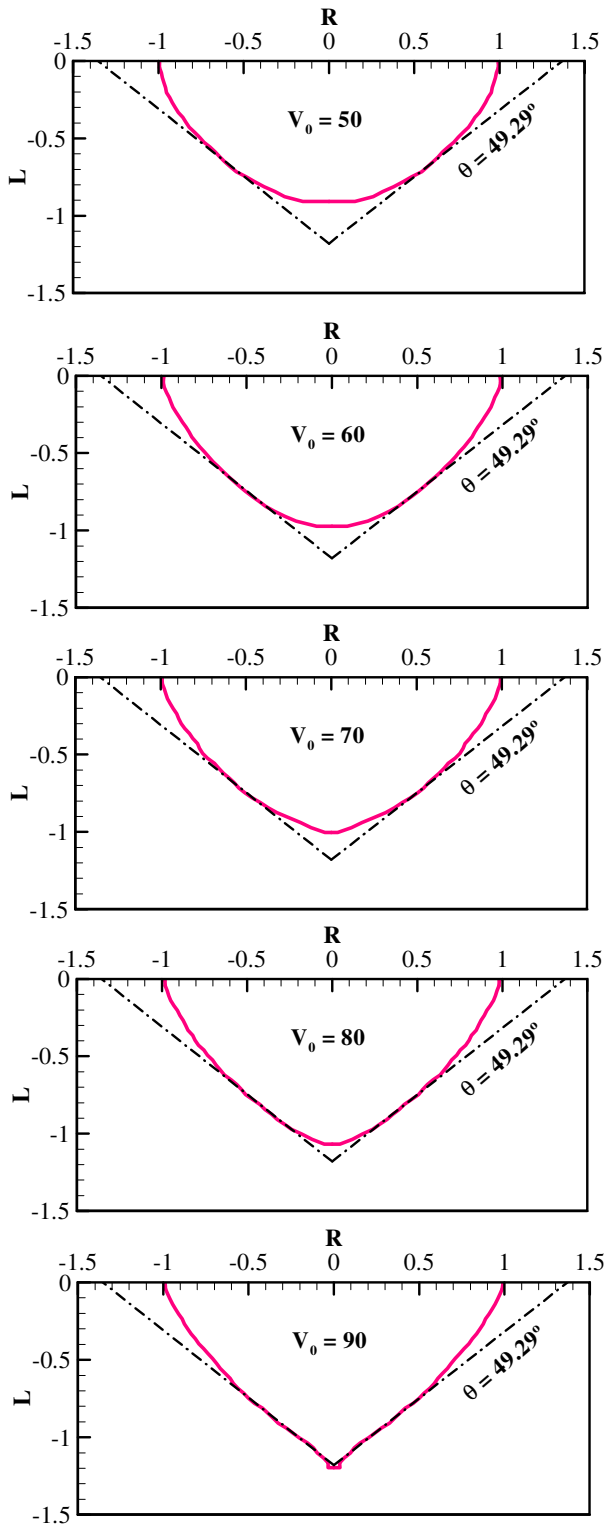


Figure 6: Dynamic response of a static drop subjected to the electrical field with different strengths

Table 2: Fluid properties in DPD and physical units

	MDPD	Physics
Density	6	$1000 \text{ kg} / \text{m}^3$
W-A* Surface tension	7.53	$0.072 \text{ N} / \text{m}$
Viscosity	5.33	$10^{-3} \text{ Pa}\cdot\text{s}$
Drop radius	10.0	R
Ohnesorge number	0.25	$1.178 \times 10^{-4} / \sqrt{R}$

*Air

Fig. 7 shows the dimensionless ratio $L_d = L/R$ versus the electrical Bond number $N_e = \epsilon V^2 / 2R\Gamma$. L is the length of the drop tip with respect to the base and R is the base radius. The results of Notz and Basaran [18], are depicted in this figure also. They numerically simulated the Taylor cone in the macroscale regime. The results of our simulation are in good agreement with their results. The fluctuations appeared in the DPD results in Fig. 7 come from the fact that the present simulation corresponds to a mesoscale problem in which thermal motions is important.

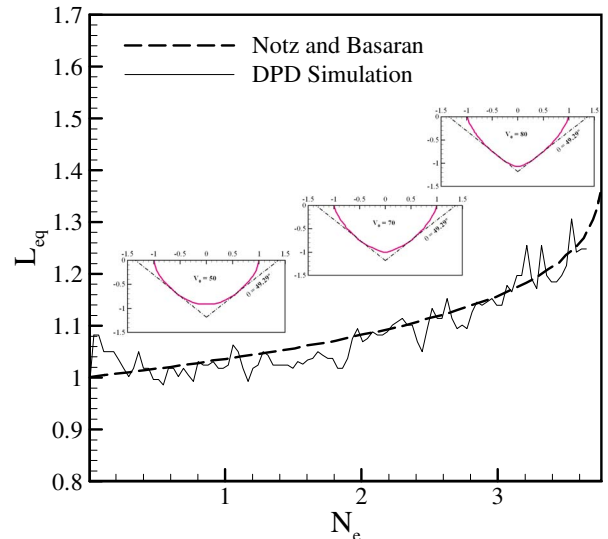


Figure 7: dimensionless length ratio as a function of electrical Bond number.

VI. CONCLUSION

In this work, we described a new algorithm for incorporating electrical forces into the DPD method for a free surface problem. The algorithm is based on the electrostatic assumption as the electrical relaxation time is much smaller than the DPD time scale for the perfect conductive fluids. In order to find the electrical force applied to each DPD particle, surface charge density is found by calculating electrical potential gradient at the fluid interface. Then the surface force is calculated in a cell near the interface and redistributed to the corresponding

particles resident in that cell. Finally, the electric forces are added to the other DPD forces. The electrostatic field in one DPD time step is calculated over a 3D structured uniform mesh by solving Laplace equation with a Finite Difference (FD) method.

Formation of a nanoscale Taylor cone was simulated to test the accuracy of the algorithm. The results were compared with the analytical and numerical simulations and good agreement was found for the cone shape and angle.

REFERENCES

- [1] Schlijper, A. G., Hoogerbrugge, P. J., and Manke, C. W., 1995, "Computer Simulation of Dilute Polymer Solutions with the Dissipative Particle Dynamics Method," *Journal of Rheology*, 39(3), pp. 567-579.
- [2] Boek, E. S., Coveney, P. V., Lekkerkerker, H. N. W., and Van Der Schoot, P., 1997, "Simulating the Rheology of Dense Colloidal Suspensions Using Dissipative Particle Dynamics," *Physical Review E*, 55(3), pp. 3124.
- [3] Boek, E. S., and Et Al., 1996, "Computer Simulation of Rheological Phenomena in Dense Colloidal Suspensions with Dissipative Particle Dynamics," *Journal of Physics: Condensed Matter*, 8(47), pp. 9509.
- [4] Dzwinel, W., and Yuen, D. A., 2000, "Matching Macroscopic Properties of Binary Fluids to the Interactions of Dissipative Particle Dynamics," *International Journal of Modern Physics C*, 11(1), pp. 1-25.
- [5] Groot, R. D., and Rabone, K. L., 2001, "Mesoscopic Simulation of Cell Membrane Damage, Morphology Change and Rupture by Nonionic Surfactants," 81(2), pp. 725-736.
- [6] Clark, A. T., Lal, M., Ruddock, J. N., and Warren, P. B., 2000, "Mesoscopic Simulation of Drops in Gravitational and Shear Fields," *Langmuir*, 16(15), pp. 6342-6350.
- [7] Trofimov, S. Y., Nies, E. L. F., and Michels, M. a. J., 2002, "Thermodynamic Consistency in Dissipative Particle Dynamics Simulations of Strongly Nonideal Liquids and Liquid Mixtures," *Journal of Chemical Physics*, 117(20), pp. 9383-9394.
- [8] Warren, P. B., 2003, "Vapor-Liquid Coexistence in Many-Body Dissipative Particle Dynamics," *Physical Review E*, 68(6)
- [9] Pagonabarraga, I., and Frenkel, D., 2001, "Dissipative Particle Dynamics for Interacting Systems," *Journal of Chemical Physics*, 115(11), pp. 5015-5026.
- [10] Espanol, P., and Warren, P., 1995, "Statistical-Mechanics of Dissipative Particle Dynamics," *Europhysics Letters*, 30(4), pp. 191-196.
- [11] Griffiths, D., 1999, *Introduction to Electrodynamics (3rd Edition)*, Benjamin Cummings.
- [12] Groot, R. D., 2003, "Electrostatic Interactions in Dissipative Particle Dynamics-Simulation of Polyelectrolytes and Anionic Surfactants," *Journal of Chemical Physics*, 118(24), pp. 11265-11277.
- [13] Groot, R. D., and Warren, P. B., 1997, "Dissipative Particle Dynamics: Bridging the Gap between Atomistic and Mesoscopic Simulation," *Journal of Chemical Physics*, 107(11), pp. 4423-4435.
- [14] Nikunen, P., Karttunen, M., and Vattulainen, I., 2003, "How Would You Integrate the Equations of Motion in Dissipative Particle Dynamics Simulations?," *Computer Physics Communications*, 153(3), pp. 407-423.
- [15] Taylor, G., 1964, "Disintegration of Water Drops in an Electric Field," *Proceedings of the Royal Society of London. Series A, Mathematical and Physical Sciences*, 280(1382), pp. 383-397.
- [16] Mudpack, <http://www.scd.ucar.edu/css/software/mudpack>
- [17] Eggers, J., 1997, "Nonlinear Dynamics and Breakup of Free-Surface Flows," *Reviews of Modern Physics*, 69(3), pp. 865-929.
- [18] Notz, P. K., and Basaran, O. A., 1999, "Dynamics of Drop Formation in an Electric Field," *Journal of Colloid and Interface Science*, 213(1), pp. 218-237.